Ninth International Topical Meeting on Nuclear Reactor Thermal Hydraulics (NURETH-9)
San Francisco, California, October 3 - 8, 1999.

Towards boiling crisis simulation : the level set method.

Samuel Kokh, Grégoire Allaire* and Sébastien Clerc
DRN/DMT/SERMA
CEA Saclay
91191 Gif-sur-Yvette, France
samuel.kokh@cea.fr allaire@ann.jussieu.fr sebastien.clerc@cea.fr

KEY WORDS

Level set method, two-phase flow.

ABSTRACT

The accurate prediction of the so-called Departure from Nucleate Boiling is a crucial point in the safety analysis of nuclear reactor cores. Nowadays, the DNB evaluation is based on experimental correlations using numerical results of averaged two-phase flow models. A natural goal is therefore to replace this rough procedure by a direct numerical simulation of the boiling crisis. The physical model now involves the motion of two phases separated by an interface and the main difficulty is to simulate this interface. Although there are many unresolved issues concerning the modelling of the entire boiling crisis phenomenon (such as triple points, nucleation, etc.), we focus merely on the numerical aspects of solving its hydrodynamics. Our goal is to devise a numerical algorithm for computing the motion of two compressible phases separated by an interface (with surface tension effects) through which mass, momentum, and energy exchanges occur. It is based on the level set method introduced by Osher and Sethian (1988) which views the interface as the zero level set of a so-called "level set function". Contrary to other methods, *e.g.* front tracking, the point is not to follow precisely the interface but rather to "capture" it on a fixed Eulerian mesh. The level set function is evolved by a new equation of Hamilton-Jacobi type. The main advantages of this method are its ability to deal with complex interface topologies and its versatility even for three-dimensional computations.

1 Introduction

With the evolution of computer power new challenges emerge in the numerical simulation of two-phase flows with applications to the safety analysis of nuclear reactors. Nowadays, almost all computer codes in this area are based on averaged models of two-phase flows. These models deliver satisfactory macroscopic results but are unable to predict fine microscopic phenomena that still may be pertinent for safety analysis. This is the case, for example, for the prediction of the onset of the boiling crisis in a the reactor core. Industrial computer codes use instead experimental correlations to check that nominal operating conditions stay away, with a safe margin, from the departure of nucleate boiling. The steady progress in computer speed now allows to overcome these averaged modelizations and to propose a direct simulation of the two phases separated by an interface. Many recent works

*Laboratoire d'Analyse Numérique, Université Paris-VI, 75252 Paris Cedex 5, France

have focused on the computation of such microscopic multifluid flows, using different numerical methods such as volume of fluid (VOF), front-tracking, second-gradient, or level set, see *e.g.* Chang (1996), Jamet (1998), Juric (1998), Zaleski (1994), Mulder (1992), Abgrall (1998), Smereka (1994), Tryggvason (1994). Our work pertains to the latter category, namely level set methods, which have been introduced by Osher and Sethian in (Osher, 1988).

The ultimate goal of our work is the numerical simulation of the boiling crisis, but we hasten to say that it is a long-term multidisciplinary program and that our contribution reduces to the design and testing of robust numerical methods. In a first step, we simplify the problem to focus only on algorithmic issues for the hydrodynamic simulation of the two phases. Our main simplifications are: no triple points (*i.e.*the interface never touches the boundary), no nucleation process (*i.e.*we treat film boiling or bubble growth), no phase changes (*i.e.*we consider two immiscible fluids rather than two phases of the same fluid). The latter restriction will soon be removed by introducing a supplementary condition at the interface, a so-called kinetic relation, see *e.g.* Truskinowsky (1991) that allows to determine the amount of phase change. In such a restricted setting our purpose is to propose a numerical method for computing the flow of two compressible fluids separated by an interface. It is a purely eulerian method that captures the interface on a fixed mesh and takes into account surface tension effects. It is based on the level set algorithm of Osher and Sethian (1988) and on a modelization of isothermal mixture of perfect fluids, see *e.g.* Abgrall (1996).

The level let method has already been implemented widely in the cases of incompressible fluids and has proved its ability to describe accurately the interface. However, for diphasic flows, compressibility cannot be neglected and it must be adequately implemented. On the other hand, VOF methods are very simple and efficient for computing compressible flows. However, their major drawback is that the computed interface is not accurately localized and spreads over a region where the volume fractions take intermediate values. In some sense, our method tries to combine the numerical schemes issued from VOF methods for their ability to simply describe the flow and the level set method for its capacity to localize accurately the interface. Our numerical examples are all two-dimensional, but there is no theoretical or practical difficulty to extend our method to the three-dimensional setting (an essential feature of VOF or level set methods compared to front-tracking).

2 Modelling of the two-phase flow

As already said we consider the motion of the two compressible fluids separated by an interface with an Eulerian method. Therefore, we discretize the equations of motion on a fixed mesh, and the interface will be captured, rather than tracked, on this Eulerian mesh. As for any front-capturing method, our numerical method has a tendency to diffuse the interface. In other words, instead of computing a sharp interface, we obtain a small layer of cells around the true interface in which we have a mixture of both fluids. The width of this transition layer will be controled by the level set method which acts as an anti-diffusion process. Although this transition layer has no special physical meaning, we have to model it in order to globally compute the hydrodynamics of the two fluids in the whole domain. The purpose of this section is to present our choice of model for the two-phase mixture. It is based on ideas borrowed from isothermal mixing of perfect gases, see *e.g.* (Abgrall, 1996).

Let us denote by ρ_i, c_{pi}, c_{vi}, with $i = 1, 2$ respectively the density, specific heat at constant volume and pressure of the i^{th} fluid. If we note T_i, its temperature, p_i, its partial pressure and ε_i, its specific internal energy, we have

$$p_i = \rho_i r T_i \quad , \quad \varepsilon_i = c_{vi} T_i.$$

During the computation, there will be cells containing both fluids, and we need to define a new equation of state for this mixture if we want to treat it as a single equivalent fluid. This is a purely numerical artefact and we emphasize that it has no real physical meaning. We make the assumption of a thermal equilibrum, *i.e.*in the area where both species are present, they share the same temperature T. Furthermore, we also make the assumption that the pressure is given by Dalton's law.

Let $\rho = \rho_1 + \rho_2$ be the density of the mixture and $c_i = \rho_i / \rho$ the mass fraction of the i^{th} gas. If we note ε, and p, respectively the specific internal energy and the pressure of the mixture, altogether our assumptions imply

$$\rho\varepsilon = \sum_i \rho_i \varepsilon_i, \quad p = \sum_i p_i. \tag{1}$$

Introducing thermodynamic parameters for the mixture

$$c_p = c_1 c_{p1} + c_2 c_{p2}, \tag{2}$$
$$c_v = c_1 c_{v1} + c_2 c_{v2}, \tag{3}$$
$$\gamma = \frac{c_1 c_{p1} + c_2 c_{p2}}{c_1 c_{v1} + c_2 c_{v2}}, \tag{4}$$

those values allow us to rewrite (1) as

$$\varepsilon = c_v T, \quad p = (\gamma - 1)\rho\varepsilon. \tag{5}$$

Therefore, the mixture state equation is similar to that of a perfect gas, except that the γ parameter depends on the mass fractions. This mixing process can be applied to wider classes of gas, *e.g.* stiffened gas (Abgrall, 1998). For real gas, one can use an equivalent-γ for the mixture. Moreover, there are other possible mixing laws which could help us to define a state equation for the mixture. In any case, the purpose of our modelization is to view the mixture zone (as well as the entire domain) as occupied by a single equivalent fluid.

The other notations in this article are the specific total energy of the mixture, $e = \varepsilon + (u^2 + v^2)/2$, and the fluid mixture velocity $\vec{u}$ of components (u, v). For the sake of simplicity, we also define two parameters

$$\kappa = \gamma - 1 \text{ and } \xi = \frac{1}{\kappa}. \tag{6}$$

Neglecting for the moment all diffusive effects and source terms, the equations of motion for the equivalent fluid are the mass, momentum, and energy conservation laws, which read in 2 dimensions as

$$\frac{\partial U}{\partial t} + \frac{\partial F(U)}{\partial x} + \frac{\partial G(U)}{\partial y} = 0 \tag{7}$$

with U the vector of conservative variables and $F(U), G(U)$ the fluxes

$$U = \begin{pmatrix} \rho_1 \\ \rho_2 \\ \rho u \\ \rho v \\ \rho e \end{pmatrix}, \qquad F(U) = \begin{pmatrix} \rho_1 u \\ \rho_2 u \\ \rho u^2 + p \\ \rho uv \\ (\rho e + p)u \end{pmatrix}, \qquad G(U) = \begin{pmatrix} \rho_1 v \\ \rho_2 v \\ \rho uv \\ \rho v^2 + p \\ (\rho e + p)v \end{pmatrix}. \tag{8}$$

This formulation allows us, through discretization to write a conservative numerical scheme that will bedescribed in the next section.

3 Numerical method

3.1 Discretized System

For the sake of simplicity, we restrict our presentation to the one dimensional case. Thus we have now instead of (7) the following system

$$\frac{\partial U}{\partial t} + \frac{\partial F(U)}{\partial x} = 0 \tag{9}$$

with

$$U = \begin{pmatrix} \rho_1 \\ \rho_2 \\ \rho u \\ \rho e \end{pmatrix}, \qquad F(U) = \begin{pmatrix} \rho_1 u \\ \rho_2 u \\ \rho u^2 + p \\ (\rho e + p)u \end{pmatrix} \qquad . \tag{10}$$

This system is discretized in the following way

$$U_i^{n+1} = U_i^n - \frac{\Delta t}{\Delta x}\left[\phi_{i+1/2}^n - \phi_{i-1/2}^n\right] \tag{11}$$

where $\phi_{i+1/2}^n$ is the numerical flux at time t_n, at the interface $(i+1/2)$ which separates the cell i and the cell $(i+1)$. In the present work we adopt the Roe scheme (Roe, 1981), (Abgrall, 1996) to solve the system. Thus the numerical flow $\phi_{i+1/2}^n$ is now expressed $\phi(U_i^n, U_{i+1}^n)$ where, considering 2 states U_L and U_R, we have

$$\phi(U_L, U_R) = \frac{1}{2}\Big[F(U_L) + F(U_R) - |A(U_L, U_R)|(U_R - U_L)\Big] \tag{12}$$

F is given by (10), and A is a matrix called Roe Matrix which depends on the states U_L and U_R, which expression will be discussed straight after.

Let us recall that given M be a diagonalisable (N, N)-matrix, given $(\lambda_i)_{i=1,N}$ and $(\vec{r_i})_{i=1,N}$ respectively the set of its real eigenvalues and eigenvectors, we denote by R the matrix which the i^{th} column is constituted of the coordinates of $(\vec{r_i})_{i=1,N}$, and $|\Lambda|$ the diagonal matrix which the i^{th} diagonal element is $|\lambda_i|$. Then $|M|$ is defined by $|M| = R|\Lambda|R^{-1}$.

3.2 Roe Matrix

According to (Roe, 1981)

$$A(U_L, U_R) = \mathrm{d}F(U^*)$$

where F is given by (10), $\mathrm{d}F$ stands for its Jacobian, and U^* is some "average state" depending on U_L and U_R which must verify

$$F(U_R) - F(U_L) = \mathrm{d}F(U^*)(U_R - U_L).$$

Let us first write the Jacobian of F, with the following notations

$$\chi_i = \left(\frac{\partial p}{\partial \rho_i}\right)_{\rho_j, \rho\varepsilon}, \qquad \beta_i = \chi_i + \kappa\frac{u^2}{2}. \tag{13}$$

We have

$$\mathrm{d}F(U) = \begin{pmatrix} u(1-c_1) & -uc_1 & c_1 & 0 \\ -uc_2 & u(1-c_2) & c_2 & 0 \\ (\beta_1 - u^2) & (\beta_2 - u^2) & (2-\kappa)u & \kappa \\ (\beta_1 - h)u & (\beta_2 - h)u & (h - \kappa u^2) & (1+\kappa)u \end{pmatrix} \tag{14}$$

Concerning the "average state "U^*, as in (Roe, 1981) we introduce the following notation

$$\overline{a} = \frac{\sqrt{\rho_L}a_L + \sqrt{\rho_R}a_R}{\sqrt{\rho_L} + \sqrt{\rho_R}}$$

It has been checked in (Abgrall, 1996) that the following values define a suitable average state U^*

$$\left\{ \begin{array}{rcl} c_i^* & = & \overline{c_i} \\ u^* & = & \overline{u} \\ h^* & = & \overline{h} \\ \kappa^* & = & \dfrac{\displaystyle\sum_i \overline{c_i} c_{vi} \kappa_i}{\displaystyle\sum_i \overline{c_i} c_{vi}} \\ \chi_i^* & = & c_{vi}(\kappa_i - \kappa^*)\overline{T} \end{array} \right.$$

The choice of the state U^* is not unique, and can even be chosed by averaging more than 2 states, which could be useful for k-points numerical schemes, $k > 2$. A drawback of this numerical scheme is that it generates some oscillations in pressure near the contact discontinuities. In the next section we will expose a method proposed by (Abgrall, 1996) to avoid this oscillation effect.

3.3 Pressure at contact discontinuities

The main idea in order to limit pressure oscillations at the interface is to find a modified numerical which preserves contact discontinuities. It means that if at time t_n, there is a real contact discontinuity between two state U_L^n and U_R^n, *i.e.* $p_L^n = p_R^n$ and $u_L^n = u_R^n$, then at

time t_{n+1} we still have a contact discontinuity between U_L^{n+1} and U_R^{n+1}: $p_L^{n+1} = p_R^{n+1}$ and $u_L^{n+1} = u_R^{n+1}$.

Recalling our notation (6), (Abgrall, 1996) has shown that the parameter γ must be discretized through the following relation

$$\xi_i^{n+1} = \xi_i^n - \frac{\Delta t}{2\Delta x}\Big(u_i^n[\xi_{i+1}^n - \xi_{i-1}^n] - |u_i^n|\,[\xi_{i+1}^n - \xi_{i-1}^n]\Big) \tag{15}$$

Indeed this equation is the discretization of the advection equation that ξ must verify

$$\frac{\partial \xi}{\partial t} + \vec{u} \cdot \overrightarrow{\text{grad}}\xi = 0 \tag{16}$$

Taking into account this relation, we can now sketch our whole numerical scheme

1. compute the intermediate state $(\hat{U})^{n+1} = (\hat{\rho}_1^{n+1}, \hat{\rho}_2^{n+1}, \widehat{(\rho u)}^{n+1}, \widehat{(\rho e)}^{n+1})$, $\hat{\rho}^{n+1} = \hat{\rho}_1^{n+1} + \hat{\rho}_2^{n+1}$ using the Roe-based scheme (11) (12);
2. compute $(\xi)^{n+1}$ with the transport equation (15);
3. compute the concentration c_i^{n+1} from (4), using: $\rho_i^{n+1} = c_i^{n+1}\hat{\rho}^{n+1}$,
4. compute the final state U^{n+1}, using:

$$\rho_i^{n+1} = c_i^{n+1}\hat{\rho}^{n+1} \quad , \quad (\rho u)^{n+1} = \widehat{(\rho u)}^{n+1} \quad , \quad (\rho e)^{n+1} = \widehat{(\rho e)}^{n+1}.$$

3.4 Level set method

So far, our numerical scheme describes the interface $\Gamma(t)$ as a thick zone as does the VOF method. In order to accurately localize the interface we implement an extra step using the level set method. The main idea (Sethian, 1988) is to introduce a function $\varphi(x,t)$ such that its zero level set is precisely the interface, *i.e.*$\varphi(x,t) = 0 \iff x \in \Gamma(t)$. Differentiating this equation and extending it to the whole domain yields a simple transport equation for the level set function φ

$$\begin{cases} \varphi(x,0) = 0 \iff x \in \Gamma(0) \\ \dfrac{\partial \varphi}{\partial t} + \vec{u} \cdot \overrightarrow{\text{grad}}\varphi = 0 \qquad \forall t > 0 \end{cases} \tag{17}$$

Given $\Gamma(0)$, the interface at $t = 0$, a common choice for the initialization $\varphi(\cdot, 0)$ of the level set function is the signed distance to the interface, *i.e.*

$$\varphi(0,x) = \begin{cases} +\text{d}(x, \Gamma(0)) & \text{if } x \text{ is in fluid 2} \\ -\text{d}(x, \Gamma(0)) & \text{if } x \text{ is in fluid 1} \end{cases} \tag{18}$$

Unfortunately, throughout the motion, φ is numerically updated by (17), and it does not stay the signed distance function to the interface $\Gamma(t)$. Because of numerical diffusion,

the slope of φ has a tendency to flatten, and the localization of its zero level set becomes increasingly unstable. An efficient remedy is to frequently re-initialize φ without changing its zero level set, *i.e.*to straighten out its front without moving the interface. This can be done (Smereka, 1994) without knowing explicitly the position of the interface, simply by solving the following Hamilton-Jacobi equation

$$\begin{cases} \dfrac{\partial \psi}{\partial s}(x,s) = \text{sign}(\psi_0)(1 - |\overrightarrow{\text{grad}}\psi|) & \forall s > 0 \\ \psi(x,0) = \psi_0(x) = \varphi(x,t_0) \end{cases} \tag{19}$$

which is known, as s goes to infinity, to admit a steady state solution which is again the signed distance function to the zero-level set of the initial condition $\varphi(x,t_0)$ (recall that the distance function $\text{d}(x,\Gamma)$ satisfies $|\overrightarrow{\text{grad}}(\text{d})(x)| = 1$). Here s can be seen as an "evolution variable" which has nothing to do with the time variable t. Thus, solving (19) is just a convenient anti-diffusion procedure for the level set function which does not change the interface position.

Remark that both equations (16) and (17) are the same transport equation for $\xi = (\gamma - 1)^{-1}$ and φ respectively. These two variables are not independent since, introducing the Heavyside function H (which is 0 on negative values and 1 on positive ones), they satisfy

$$\xi(x,t) = (\xi_2 - \xi_1)H(\varphi(x,t)) + \xi_1. \tag{20}$$

The idea is therefore to still solve equation (16) - and not (17) - and to add the anti-diffusion equation (19). Since the Heavyside function H is not continuous, we approximate it by a smooth function $\widetilde{H}$ such as $\widetilde{H}(d) = (1 + d(d^2+1)^{-1/2})/2$. It allows to recover from the values of ξ a function φ which is the initial condition of (19), and its steady state is in turn translated into a new sharp function ξ. This process is made every k time steps, the smaller k the faster the convergence in (19) (usually we take $k = 1$). Remark that it does not require the explicit knowledge of the interface localization and is therefore not too time consuming.

3.5 Second Order Extension

A convenient way to gain second order accuracy in space, consists in applying a MUSCL method to our present scheme on the classical equations of motion (9) and (10). Then, by applying the same lines as in section 3.3 we will find the order-two equivalent of the discretized advection equation for ξ. For details on the MUSCL method we refer *e.g.* to (Godlewski, 1996).

Let us step back to (12). In each cell the conservative variables are now discretized as piecewise affine, and not merely constant. Given a cell face $i+1/2$ between the cell i and the cell $i+1$, we simply introduce new expressions for the right and left states, $U^+_{i+1/2}$ and $U^-_{i+1/2}$ respectively, instead of the previous constant state U_{i+1} and U_i. To preserve the seond-order scheme from spurious oscillations, a minmod slope limiter is used. It leads to

the following expressions

$$U^+_{i+1/2} = U_{i+1} - \frac{1}{4}\left(\overline{\Delta_{i+3/2}U} + \underline{\Delta_{i+1/2}U}\right) \quad (21)$$

$$U^-_{i+1/2} = U_i + \frac{1}{4}\left(\underline{\Delta_{i-1/2}U} + \overline{\Delta_{i+1/2}U}\right) \quad (22)$$

with the notation $\Delta_{i+1/2}U = U_{i+1} - U_i$ and

$$\overline{\Delta_{i+1/2}U} = \text{minmod}(\Delta_{i+1/2}U, \Delta_{i-1/2}U), \quad (23)$$

$$\underline{\Delta_{i+1/2}U} = \text{minmod}(\Delta_{i+1/2}U, \Delta_{i+3/2}U). \quad (24)$$

This yields the second order implementation of (11). To get rid of presssure oscillations, we again need to find a suitable advection equation for the variable $\xi = (\gamma - 1)^{-1}$. A similar computation to that done in section (3.3) leads to the second order equivalent of (15)

$$\begin{aligned}\xi_i^{n+1} = \xi_i^n &- \frac{\Delta t}{2\Delta x}u_i^n\left[\xi^+_{i+1/2} + \xi^-_{i+1/2} - \xi^+_{i-1/2} - \xi^-_{i-1/2}\right] \\ &+ \frac{\Delta t}{2\Delta x}|u_i^n|\left[\xi^+_{i+1/2} - \xi^-_{i+1/2} - \xi^+_{i-1/2} + \xi^-_{i-1/2}\right]\end{aligned} \quad (25)$$

3.6 Extension to 2d

The extension to two-dimensional problems is really straightforward if cartesian structured meshes are used. The notations of this paragraph refer to those of (7) and (8). The generalization of (11) is obtained by discretizing separately in x and y, *i.e.*along the directions of the grid. It yields

$$U^{n+1}_{i,j} = U^n_{i,j} - \frac{\Delta t}{\Delta x}\left[\phi^n_{i+1/2,j} - \phi^n_{i-1/2,j}\right] - \frac{\Delta t}{\Delta y}\left[\theta^n_{i,j+1/2} - \theta^n_{i,j-1/2}\right] \quad (26)$$

where $\phi^n_{i+1/2,j}$ is the numerical flux at time t_n, at the interface $(i+1/2, j)$ which separates the cell (i, j) and the cell $(i+1, j)$, and $\theta^n_{i,j+1/2}$ is the numerical flux at time t_n, at the interface $(i, j+1/2)$ which separates the cell (i, j) and the cell $(i, j+1)$.

As before, we have $\phi^n_{i+1/2,j} = \phi(U^n_{i,j}, U^n_{i+1,j})$, with $\phi(U_L, U_R)$ defined as in section 3.1. A similar definition is set for θ using the flux G (as defined in (8) and its corresponding Roe matrix B. Thus we have $\theta^n_{i,j+1/2} = \theta(U^n_{i,j}, U^n_{i,j+1})$, using $\theta(U_L, U_R)$ defined by

$$\theta(U_L, U_R) = \frac{1}{2}\Big[G(U_L) + G(U_R) - |B(U_L, U_R)|(U_R - U_L)\Big]. \quad (27)$$

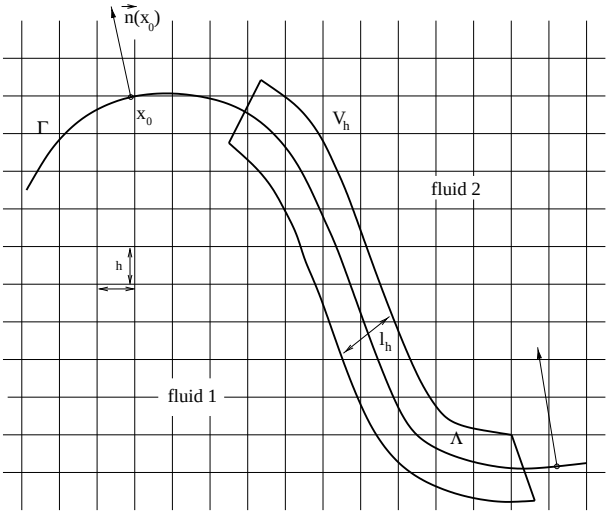

Fig. 1: surface tension.

4 Surface tension

4.1 Continuum surface tension model

The surface tension is a macroscopic effect of a localized microscopic force that acts on fluid elements at the interface. Although the interface is not material, it gives it some elastic properties. As in (Brackbill, 1992), we express the surface tension as a surface force per unit of area localized at the interface, with the following form

$$\vec{F}(x_0) = \sigma \mathcal{C}(x_0)\vec{n}(x_0)$$

where σ stands for the fluid surface tension coefficient (in units of force per unit length), x_0 is a point on the interface, $\vec{n}(x_0)$ is the unit normal to the interface at the point x_0 directed from fluid 1 to fluid 2, $\mathcal{C}(x)$ is the local curvature at x_0, which is positive when the center of curvature is in fluid 2.

In our numerical scheme the interface is artificially spread out by numerical diffusion. We thus approximate this surface force by a volume force which tends to the surface force $\vec{F}$ as the thickness of the interface tends to 0. In other words, the surface tension is seen as a continuous body force across the interface. Let h denotes the resolution of the grid, ξ_h be the piecewise constant approximation of ξ

$$\lim_{h\to 0} \overrightarrow{\mathrm{grad}}\,\xi_h(x) = \vec{n}(x)[\xi]\delta_\Gamma(x)$$

where $[\xi] = \xi_2 - \xi_1$, and δ_Γ is the Dirac distribution localized on the interface Γ between both fluids.

Let Λ be a portion of the interface, and V_h a volume which includes Λ. We assume that its edges are normal to Λ and that it has a constant thickness $l_h > 0$ (cf. figure 1). The resultant of the surface tension forces acting on Λ is

$$\mathcal{F} = \int_\Lambda \vec{F}(x)\mathrm{d}S = \int_{V_h} \vec{F}\delta_\Gamma(x)\mathrm{d}\tau = \int_{V_h} \sigma\mathcal{C}(x)n(x)\delta_\Gamma(x)\mathrm{d}\tau$$

We define the volume force $\vec{F}_h$ by

$$\vec{F}_h(x) = \sigma \mathcal{C}(x) \frac{1}{[\xi]} \overrightarrow{\mathrm{grad}} \xi(x)$$

If l_h is chosen in such a way that $h < l_h < Mh$, with a given positive constant $M > 0$, we obtain

$$\lim_{h \to 0} \int_{V_h} \vec{F}_h(x) \mathrm{d}\tau = \int_{\Lambda} \vec{F}(x) \mathrm{d}S = \mathcal{F}.$$

Therefore, the volume force $\vec{F}_h$ has the desired property that, in the limit of zero-thickness of the interface, its resultant in V_h is exactly $\mathcal{F}$, when $h \to 0$.

4.2 Discretization of the surface tension

We have to find an approximate value of $\vec{F}_h$ in each cell (i, j) of the domain. Recall that

$$\vec{F}_h(x) = \sigma \mathcal{C}(x) \frac{1}{[\xi]} \overrightarrow{\mathrm{grad}} \xi \tag{28}$$

Defining $\vec{m} = (m^x, m^y) = \overrightarrow{\mathrm{grad}} \xi$, the outward unit normal to the interface is $\vec{n} = \frac{\vec{m}}{|\vec{m}|}$. Since the curvature is $\mathcal{C} = -\mathrm{div}(\vec{n})$, it satisfies

$$\mathcal{C} = \frac{1}{|\vec{m}|} \left[\left(\frac{\vec{m}}{|\vec{m}|} \cdot \overrightarrow{\mathrm{grad}} \right) |\vec{m}| - \mathrm{div}(\vec{m}) \right]. \tag{29}$$

As in (Brackbill, 1992) we use an ALE-like scheme to discretize (28) and (29) and obtain the desired discrete values $(\vec{F}_h)_{i,j}$ in each cell (i, j). In the sequel, the subscript (i, j) denotes a value at the center of the cell (i, j), while $(i, j + 1/2)$ or $(i + 1/2, j)$ stands for a value at the interface of cells, and $(i + 1/2, j + 1/2)$ is a value at a vertex (cf. figure 2).

Vertex-centered normal vectors are thus defined by

$$\begin{aligned} \vec{m}_{i+1/2,j+1/2} &= \frac{1}{2\Delta x} \left[\xi_{i+1,j} + \xi_{i+1,j+1} - \xi_{i,j} - \xi_{i,j+1} \right] \vec{e}_x \\ &\quad + \frac{1}{2\Delta y} \left[\xi_{i,j+1} + \xi_{i+1,j+1} - \xi_{i,j} - \xi_{i+1,j} \right] \vec{e}_y \end{aligned} \tag{30}$$

and cell-centered normal vectors are obtained by averaging the vertex values

$$\vec{m}_{i,j} = \frac{1}{4} (\vec{m}_{i+1/2,j+1/2} + \vec{m}_{i+1/2,j-1/2} + \vec{m}_{i-1/2,j+1/2} + \vec{m}_{i-1/2,j-1/2}).$$

The curvature $\mathcal{C}_{i,j}$ is obtained from (29) by using the following discretizations

$$\begin{aligned} (\mathrm{div}(\vec{m}))_{i,j} &= \left(\frac{\partial m^x}{\partial x} \right)_{i,j} + \left(\frac{\partial m^y}{\partial y} \right)_{i,j} \\ &= \frac{1}{2\Delta x} \left(m^x_{i+1/2,j+1/2} + m^x_{i+1/2,j-1/2} - m^x_{i-1/2,j+1/2} - m^x_{i-1/2,j-1/2} \right) \\ &\quad + \frac{1}{2\Delta y} \left(m^y_{i+1/2,j+1/2} + m^y_{i-1/2,j+1/2} - m^y_{i+1/2,j-1/2} - m^y_{i-1/2,j-1/2} \right) \end{aligned}$$

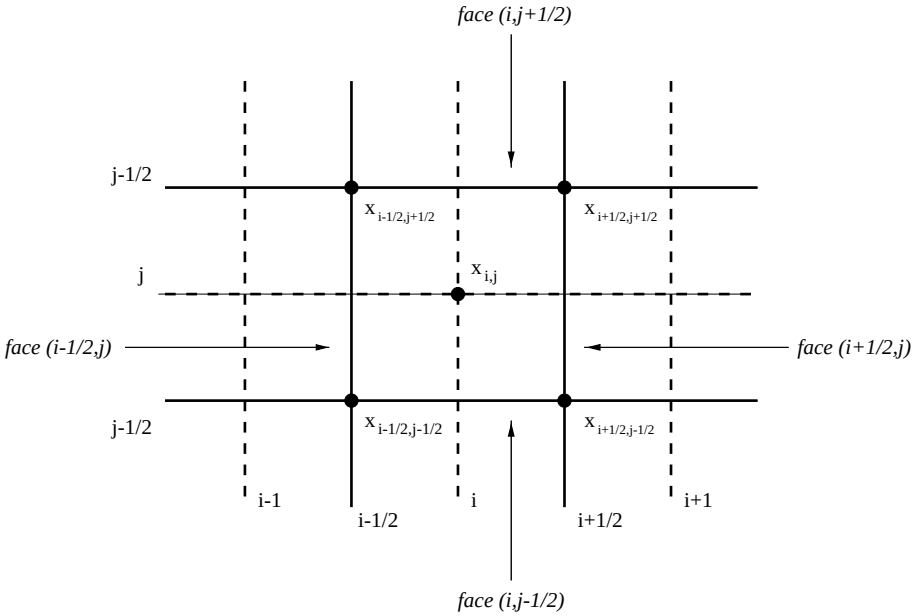

Fig. 2: grid.

and

$$\left[\left(\frac{\vec{m}}{|\vec{m}|}\cdot\overrightarrow{\mathrm{grad}}\right)|\vec{m}|\right]_{i,j} = \frac{m_{x,i,j}}{|\vec{m}_{x,i,j}|}\left(\frac{\partial|\vec{m}|}{\partial x}\right)_{i,j} + \frac{m_{y,i,j}}{|\vec{m}_{y,i,j}|}\left(\frac{\partial|\vec{m}|}{\partial y}\right)_{i,j}.$$

5 Numerical results

5.1 Shock tube

Our first test case is a bifluid shock tube. The computation is one dimensional, and at the initial time the left part of the tube contains helium under high pressure, while the right side of the tube is filled with air at atmospheric pressure (see table 1). This allows us to see how well the scheme limits pressure oscillations at the contact discontinuity. Remark that the ratio between the two fluid densities is already larger than 10 (Abgrall, 1996).

The shock tube is 1m long and the mesh used here has 100 cells. We present both first order scheme and second order. Figures 3 and 4 show respectively the graph of $1/\kappa$ and pressure at time $t = 0.25$ms. The first order scheme result is represented by the plain line, as the second order one corresponds to the dashed line.

We can thus check that the oscillations have been successfully removed from the pressure. The MUSCL technique contribution has allowed to sharpen all fronts compared to the first order computation where the interface is rather smeared.

Table 1: Initial state of the shock tube

	ρ (kg.m^{-3})	u (m.s^{-1})	v (m.s^{-1})	p (Pa)	γ	c_p (J.kg^{-1}.K^{-1})	c_v (J.kg^{-1}.K^{-1})
Left side (helium)	14.54903	0	0	194×10^5	1.67	4041.4	2420
Right side (air)	1.16355	0	0	10^5	1.4	1024.8	732

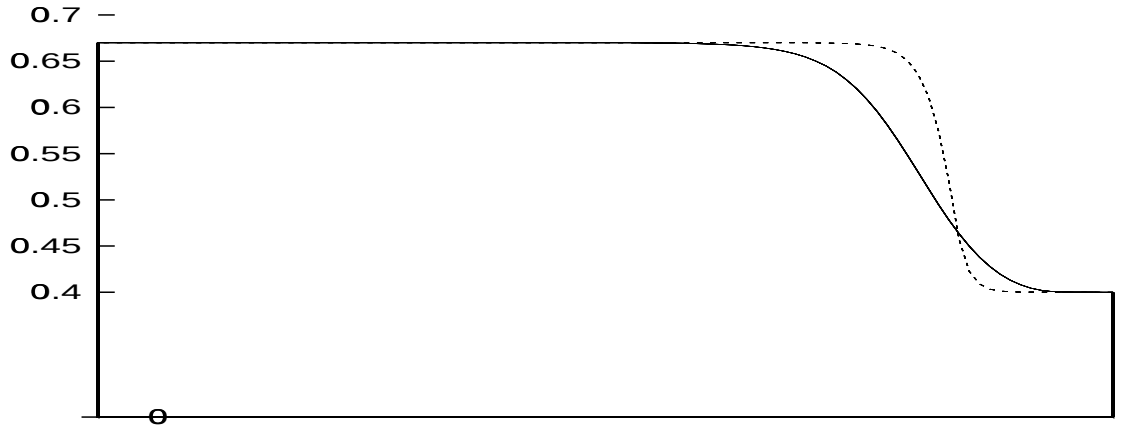

Fig. 3: graph for κ, first and seconder order

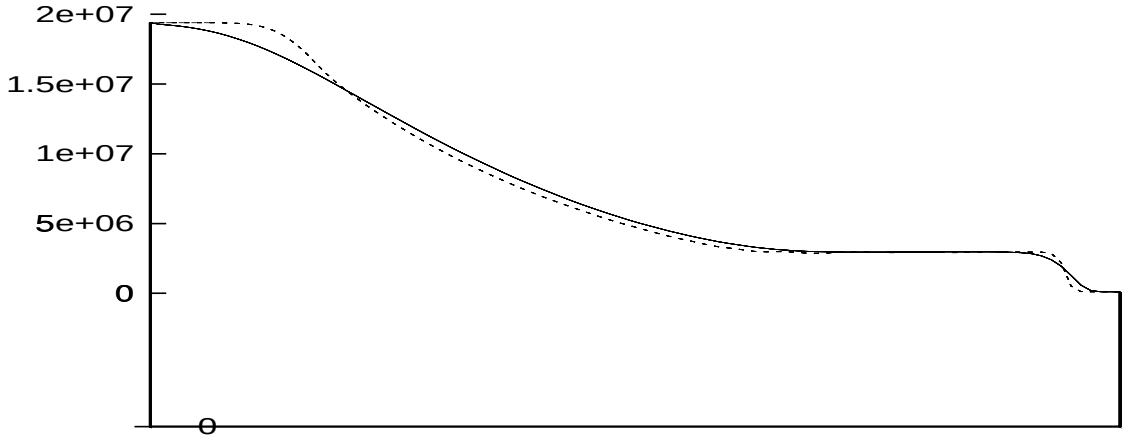

Fig. 4: graph for pressure, first and seconder order

5.2 Shock in an helium bubble

Our second test case is a two-dimensional simulation of a shock hitting an helium bubble surrounded by air (for references, see (Abgrall, 1996), (Karni, 1994)). The shock travels from the left to the right of the domain at a constant speed before it hits the bubble. In front of the shock, the helium bubble and the surrounding air are in equilibrium having the same pressure (see table 2). The domain is a square of side 1m, and we use a regular mesh of 200×200 cells. At time $t = 0$, the shock wave is located at $x = 0.25$m, the bubble diameter is 0.2m and its center sits at $(x, y) = (0.5\text{m}, 0.5\text{m})$. The value used for the fluid surface tension coefficient σ is here $23.61 \times 10^{-4} N.m^{-1}$.

Table 2: Initial state of the shock tube with the helium bubble

location	ρ (kg.m^{-3})	u (m.s^{-1})	v (m.s^{-1})	p (Pa)	γ	c_p (J.kg^{-1}.K^{-1})	c_v (J.kg^{-1}.K^{-1})
air after shock	1.3765	0.3948	0	1.57	1.4	1024.8	732
air before shock	1	0	0	1	1.4	1024.8	732
helium before shock	0.138	0	0	1	1.67	4041.4	2420

The final time is $t = 0.35$s. Figure 6 displays the discontinuity of the κ parameter, *i.e.*the shape of the bubble along with some level-set lines of the pressure in a small "window" which encloses the bubble position. Each "shot" corresponds to successive times increased by $\Delta t = 0.035$s. At $t = 105$ms the shock wave hasn't reach the bubble yet, then at $t = 140$ms the back of the bubble begins to flatten and the bubble step by step looses its circular shape.

The figure 5 displays the pressure at time $t = 0.35$s. Although the shock is now beyond the bubble, it remains in the post shock zone a circular pressure gap. This singularity corresponds to the helium bubble which, after the shock, is not any longer in pressure equilibrium with the surrounding air. The position of the shock wave appears on figure 5 as a vertical line. Notice that thanks to the MUSCL method the front of the shock waves remains sharp (see 5).

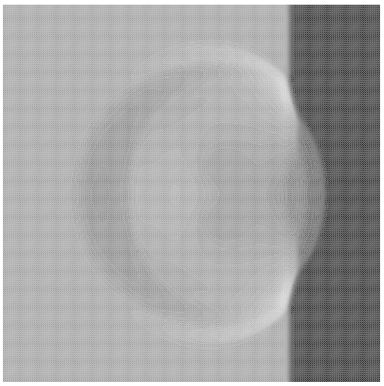

Fig. 5: pressure values at $t = 0.35$s

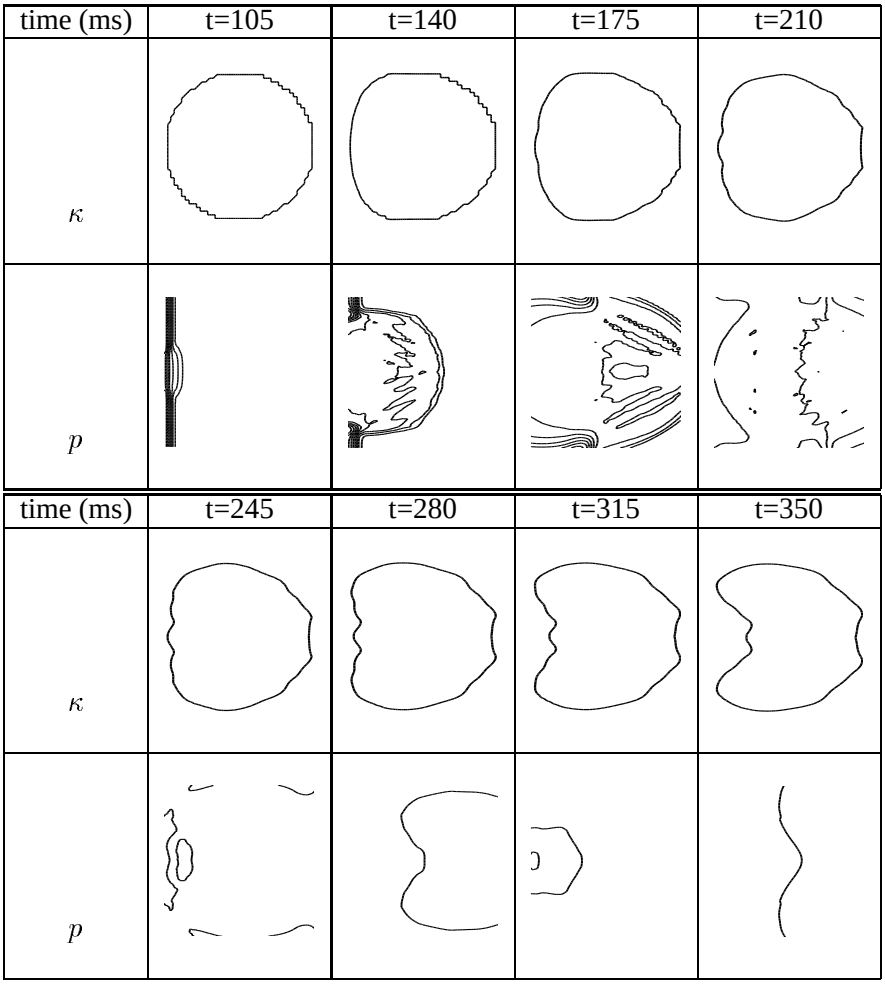

Fig. 6: pressure and κ level-set graph

6 Conclusion and perspectives

We have developed a numerical scheme for computing the motion of two compressible fluids separated by an interface. Surface tension effects are taken into account and a level set method is used to straighten out the interface. There are many unresolved issues before we can simulate boiling crisis (our ultimate goal), but we shall focus mainly on numerical ones. The next steps in our work are the introduction of phase change by using a kinetic relation at the interface, as described *e.g.* in (Truskinowsky, 1991), the treatment of heat sources, such as a conducting wall, and further testing of the scheme robustness (especially in the case of a high ratio of the two phases densities).

REFERENCES

[Abgrall, 1996] R. Abgrall *How to prevent pressure oscillations in multicomponent flow calculations: a quasi conservative approach,* J. Comp. Phys. 125, pp.150–160.

[Brackbill, 1992] J. Brackbill, D. Kothe,C. Zemach, *A continuum method for modeling surface tension,* J. Comp. Phys. 100, pp.335–354.

[Chang, 1996] Y. Chang, T. Hou, B. Merriman, S. Osher, *A level set formulation of eulerian interface capturing methods for incompressible fluid flows,* J. Comp. Phys. 124, pp.449-464.

[Godlewski, 1996] E. Godlewski, P.A. Raviart, *Numerical approximation of hyperbolic systems of conservation laws,* Springer, New York.

[Hirt, 1981] C. Hirt, B. Nichols, *Volume of fluid (VOF) method for the dynamics of free boundaries,* J. Comp. Phys. 39, pp.201–225.

[Jamet, 1998] D. Jamet, *Etude des potentialités de la théorie du second gradient pour la simulation numérique directe des écoulements liquide-vapeur avec changement de phase,* PhD Thesis, Ecole Centrale Paris.

[Juric, 1996] D. Juric, G. Tryggvason, *Direct numerical simulations of flows with phase change,* AIAA Technical report, 96-0857.

[Juric, 1998] D. Juric, G. Tryggvason, *Computations of boiling flows,* Int. J. Multiphase Flow, 24 (3), pp.387–410.

[Karni, 1994] S. Karni, *Multicomponent flow calculations by a consistent primitive algorithm,* J. Comp. Phys. 112, pp.31–43.

[Mulder, 1992] W. Mulder, S. Osher, J. Sethian, *Computing interface motion in compressible gas dynamics,* J. Comp. Phys. 100, pp.209–228.

[Osher, 1988] S. Osher, J. Sethian, *Fronts propagating with curvature-dependent speed: algorithms based on Hamilton-Jacobi formulations,* J. Comp. Phys. 79, pp.12–49.

[Roe, 1981] P.L. Roe, *Approximate Riemann solvers, parameter vectors, and difference schemes,* J. Comput. Phys. 43, pp.357–372.

[Saurel, 1998] R. Saurel, R. Abgrall, *A simple method for compressible multifluid flows,* to appear in SIAM J. Num. Anal. .

[Sethian, 1996] J. Sethian, *Level set methods,* Cambridge University Press (1996).

[Smereka, 1994] M. Sussman, P. Smereka, S. Osher, *A level set method for computing solutions to incompressible two-phase flows,* J. Comp. Phys. 114, pp.146–159.

[Truskinowsky, 1991] L. Truskinwosky, *Kinks versus shocks,* in Shock induced transitions and phase structures In: general media, R. Fosdick et al. eds., Springer Verlag, Berlin.

[Tryggvason, 1994] S. Unverdi, G. Tryggvason, *A front-tracking method for viscous incompressible multi-fluid flows,* J. Comp. Phys. 100, pp.25–37.

[Zaleski, 1994] B. Lafaurie, C. Nardone, R. Scardovelli, S.Zaleski,G. Zanetti, *Modelling merging and fragmentation in multiphase flows with SURFER,* J. Comp. Phys. 113, pp.134–147.